STEM CELLS AND DEVELOPMENT
Volume 23, Number 16, 2014

DOI: 10.1089/scd.2014.0023

Activation of Neural Cell Fate Programs Toward Direct Conversion of Adult Human Fibroblasts into Tri-Potent Neural Progenitors Using *OCT-4*

Ryan R. Mitchell,[1,2] Eva Szabo,[1] Yannick D. Benoit,[1] Daniel T. Case,[3] Rami Mechael,[1,2] Javier Alamilla,[4] Jong Hee Lee,[1] Aline Fiebig-Comyn,[1] Deda C. Gillespie,[3,4] and Mickie Bhatia[1,2]

Several transcription factors and methods have been used to convert fibroblasts directly to neural fate and have provided insights into molecular mechanisms as to how each of these required factors orchestrate neural fate conversion. Here, we provide evidence and detailed characterization of the direct conversion process of primary adult human fibroblasts (hFib) to neural progenitor cells (NPC) using *OCT4* alone. Factors previously associated with neural cell fate conversion were induced during hFib-NPC$^{OCT\text{-}4}$ generation, where *OCT-4* alone was sufficient to induce neural fate conversion without the use of promiscuous small-molecule manipulation. Human Fib-NPC$^{OCT\text{-}4}$ proliferate, express neural stem/progenitor markers, and possess developmental potential that gives rise to all three major subtypes of neural cells: astrocytes, oligodendrocytes, and neurons with functional capacity. We propose a deconvoluted reprogramming approach for neural fate conversion in which *OCT4* is sufficient for inducing neural conversion from hFib for disease modeling as well as the fundamental study of early neural fate induction.

Introduction

Direct conversion transcription factor reprogramming of somatic cells holds great potential for the generation of patient-specific disease models, and possibly cells for transplantation therapy. Although first reported in the 1980s [1], this reprogramming method has been the basis for a plethora of studies, all of which achieve alteration of cell fate in the absence of establishing pluripotency [2–4]. The catalyzing study which resulted in the revisiting of direct conversion/transdifferentiation methods demonstrated that the expression of neural lineage-associated transcription factors in mouse fibroblasts leads to the activation of endogenous neural genes [5]. Through a process of elimination, *Brn-2, Myt1-l,* and *Ascl-1* were identified as a key set of factors that could initiate a change in cell fate from fibroblast to functional neuron (iN), in the presence of neural supportive culture conditions [5]. Soon after, with the addition of *NEUROD1,* this same combination of genes was found to induce direct conversion of human fibroblasts (hFib) to neurons. Generation of neural tissue for study or transplantation is of great value, as the physical and ethical barriers regarding biopsies of the brain are numerous. To date, the iN approach has been harnessed to produce multiple neuron subtypes by introduction of additional lineage-specific transcription factors, from both mouse and human starting cell populations of varied tissue origin [6–10]. In addition to directly converting somatic cells to postmitotic neurons, Kim et al. demonstrated the conversion of mouse fibroblasts to neuronal progenitor cells. This transformation was achieved through a brief expression of pluripotency transcription factors followed by the addition of neural supportive culture conditions [11]. Many groups have adapted this strategy by expressing the pluripotency factors alone, or in combination with neural lineage-specific factors to produce both mouse- and human-induced neural progenitor cells (iNPCs) [12–15]. iNPCs are capable of proliferating and differentiating to all three families of neural cells, including neurons, astrocytes, and oligodendrocytes. Despite the large number of studies demonstrating the direct conversion of somatic cells to NPCs, the reprogramming mechanism behind these cellular transformations remains to be completely understood. Here, we demonstrate the direct conversion of adult hFib to NPCs through the use of a single factor *OCT4*, and provide insights into the minimal essential mechanisms of reprogramming induction.

Materials and Methods

Cell culture

Dermal skin biopsies (5×5 mm) were obtained from the forearm of consenting donors in accordance with Research

[1]Faculty of Health Sciences, Stem Cell and Cancer Research Institute, [2]Department of Biochemistry and Biomedical Sciences, [3]Neuroscience Graduate Program, Department of Medicine, and [4]Department of Psychology, Neuroscience and Behavior, McMaster University, Hamilton, ON, Canada.

Ethics Board-approved protocols at McMaster University. Primary hFib cultures were established as described [16]. Human dermal adult fibroblasts (Sciencell and Donor derived) were initially maintained in fibroblast medium: DMEM (Gibco) supplemented with 10% v/v FBS (Neonatal Bovine Serum; HyClone), 1 mM L-glutamine (Gibco), and 1% v/v nonessential amino acids (NEAA; Gibco) before transduction with OCT4 lentivirus vector.

Cell viability

Viable cells were determined by Trypan Blue exclusion assay that was performed using a Countess automated cell counter (Life Technologies).

Lentivirus preparation and transduction

pSIN-EF1α-OCT4-Puro [or pHIV-EF1α-IRES-eGFP (Addgene 21373) subcloned with *OCT4* sequence from Addgene 16579] was obtained (Addgene 16579) and co-transfected with pMD2.G (Addgene 12259) and psPAX2 (Addgene 12260) plasmids into the 293-FT cell line (Invitrogen) in order to initiate virus particle production. Viral supernatants were harvested at 48 h after transfection and ultracentrifuged to concentrate the virus. hFib were transduced in 50% Fibroblast medium: 50% reprogramming medium [F12 DMEM 20% Knockout Serum Replacement (Gibco), L-glutamine (Gibco), and 1% v/v nonessential amino acids (NEAA; Gibco), 0.1 mM beta-mercaptoethanol, 16 ng/mL basic fibroblast growth factor (bFGF), 30 ng/mL insulin growth factor 2 (IGF2), supplemented with 8 μg/mL polybrene (SIGMA)].

Reprogramming, neural progenitor and differentiation culture

Adult hFib were seeded on tissue culture-treated plates at $\sim 2 \times 10^4$ cells per well of a six-well standard plate. Fibroblasts were transduced in 50% fibroblast media: 50% reprogramming media containing 8 μg/mL polybrene with sufficient *eGFP* or *OCT4* expressing lentivirus to achieve ~20% transduction efficiency as measured by flow cytometry for *eGFP* or *OCT4*, respectively. hFib expressing *eGFP* and/or *OCT4* were cultured for 8 days post transduction in reprogramming media before being trypsinzed and seeded as single cells in ultra-low attachment plates at a concentration of 1×10^5 cells per mL of progenitor culture media: F12:DMEM supplemented with 1× N2 and 1× B27 20 ng/mL bFGF, 20 ng/mL epidermal growth factor. Spheres were fed fresh media and growth factors after 7 days of culture. After 14 days, sphere clusters were dissociated using Accutase (Gibco) and seeded onto POLY-L-ORNATHINE/Mouse laminin-coated tissue culture plates in neural progenitor media for continued maintenance or in differentiation culture media consisting of F12 DMEM 1XN2 1XB27. For best differentiation, cells were cultured adherently in progenitor media until dense colony clusters appeared such as those depicted in Fig. 1K before passaging into differentiation conditions. For neuronal differentiation, media was supplemented with 5 nM forskolin. For Astrocyte differentiation, media was supplemented with 5% FBS. For Oligodendrocyte differentiation, media was supplemented with 100 ng/mL insulin growth factor 1 (IGF1), 200 nm Ascorbic Acid (Sigma), and 5 nM forskolin (Tocris). NSC from H9 were derived and cultured as previously described [17].

Flow cytometry

Intracellular staining for OCT4 [BD OCT3/4-PE(1:100), OCT3/4-647(1:100)], SOX2 [BD SOX2-647(1:1,000)], Ki67 [BD Ki67-PE(1:400)], and Live Dead Discrimination Dye [BD LiveDeadViolet (1:7,500)] was performed on cells having undergone fixation and permeablization using the BD Fix/Perm kit. Briefly, cells were washed in phosphate-buffered saline (PBS) and stained for 30 min at 4°C in LiveDeadViolet. Cells were then washed in PBS and fixed for 20 min at 4°C in Fix solution. Cells were then washed in Perm solution, and left to block in Perm solution for 1 h at 4°C. Cells were stained overnight at 4°C, before washing in PBS and acquisition. Live cell visualization of eGFP expression was performed on cells treated with 7AAD [BD (1:50)] live dead discriminator. Acquisition was performed using LSRII (BD Biosciences), and analysis was performed using FlowJo 9.2 Software.

Immuncytochemistry

For surface marker staining, cells were stained directly in PBS 3% FBS or fixed using BD Fixation buffer for 40 min 4°C. Cells were washed in 3% FBS HBSS (Gibco). For intracellular staining, cells were fixed using BD Fixation/Permeabilization buffer for 40 min at 4°C. Cells were washed in BD 1× Perm solution. Neural lineage cells were identified by staining with monoclonal antibodies OCT4-PE (BD), SOX2-647 (BD), SOX2 anti-human (BD), Nestin anti-Human (R&D), Beta-III Tubulin/Tuj1 anti-Human (R&D), Microtubule-associated protein 2/MAP2 anti-Human (Abcam), Oligodendrocyte marker 4/O4 anti-Human (R&D), Glial fibrilliary acidic protein/GFAP anti-Human (SIGMA), and CD133-PE (Miltenyi). Antibodies were diluted in BD 1× wash buffer and incubated overnight at 4°C. Nonconjugated antibodies were visualized using appropriate Alexa-Flour secondary reagents (Life Technologies). Optimal working dilutions were determined for individual antibodies.

Teratoma assay

5×10^5 iPSCs or hFib-NPC^{OCT4} were injected intratesticularly into male NOD/SCID mice. Teratomas/testis were extracted at 10–12 weeks after the injection and analyzed as previously described [17]. Samples were stained with Hematoxylin-Eosin and OCT4, mounted using Permount, and imaged by scanning slides using Aperio Scan Scope. Tissue typing was performed based on stringent histological and morphological criteria that were specific for each germ-layer subtype. The presence of the germ layers and tissue typing was confirmed by the McMaster Pathology department.

Quantitative polymerase chain reaction

Total RNA was isolated using the Qiagen mini RNA isolation kit. RNA was then subjected to cDNA synthesis using superscript III (Invitrogen). Quantitative PCR (qPCR) was performed using Platinum SYBR Green–UDP mix (Invitrogen). Threshold was set to the detection of Gus-B (β-glucuronidase)[46] and then normalized to GAPDH. Primer Sequences: ASCL1: 5′ caagagagcgcagccttag, 5′ gcaaaagtcag

tgctgaacg BRN-2: 5′ aataaggcaaaaggaaagcaact, 5′ caaaac acatcattacacctgct MYT1L: 5′ caatggaaagggattttaagca, 5′ tttg agattatgtaccaacgttagatg NEUROD1: 5′ gttattgtgttgccttagc acttc, 5′ agtgaaatgaattgctcaaattgt MSI2: 5′ ggcagcaagagga tcagg. 5′ccgtagagatcggcgaca NCAN: 5′ gccttgggccttttgatgc, 5′ ccttggtccactttatccgagg COL1A1: 5′ gagggccaagacgaagac atc, 5′ cagatcacgtcatcgcacaac DKK3: 5′ aggacacgcagcaca aattg, 5′ ccagtctggttgttggttatctt SNAI1: 5′ tcggaagcctaactaca gcga, 5′ agatgagcattggcagcgag.

Cytosolic calcium imaging

Measurement of cytosolic calcium was performed by monitoring Fluo-4 fluorescence of cells, adhered to plastic 35 mm dishes or six-well plastic plates using an Olympus IX81 inverted epi-fluorescence microscope (Olympus) that was coupled to a xenon arc lamp (EXFO). Cells were washed and incubated in Hanks' balanced salt solution HBSS, supplemented with 25 mM HEPES buffer, 5.5 mM Glucose. Indicated agonists, diluted in the aforementioned solution, were washed over the cells at the indicated timepoints, using a custom applicator and an aspirator system. Fluo-4 was loaded into the cells by incubation with 1 μM Fluo-4 (Invitrogen) acetoxymethyl ester (45 min incubation followed by a 45 min period for de-esterification). Fluorescent images were collected using an intensified charge-coupled device video camera (Photometrics) every 2 s through a GFP filter cube (Semrock). Off-line analysis of the intensity pattern of Fluo-4 signal was performed in ImageJ (NIH).

Action potential/patch clamping

To determine whether cells could fire action potentials, the cells were transferred on a coverslip to an upright microscope and were continuously perfused with artificial cerebrospinal fluid (ACSF, pH 7.2) containing (in mM) 125 NaCl, 1 $MgSO_4$, 5 KCl, 1.25 KH_2PO_4, 10 dextrose, 26 $NaHCO_3$, and 2 $CaCl_2$•$2H_2O$. ACSF was heated to ~33°C and superfused with 95% O_2/5% CO_2. Electrodes for cell-attached and whole-cell voltage clamp recordings had resistances of 2–4 MΩ and were filled with a K-gluconate solution (pH 7.3) containing (in mM) 100 K-gluconate, 20 KCl, 10 Na2-phosphocreatine, 10 HEPES, 0.3 GTP-Na, and 4 ATP-Mg•3.5H20. Recordings (MultiClamp 700B or Axopatch 200B amplifier; Molecular Devices) were sampled at 5 or 10 kHz, filtered at 2 or 5 kHz, and saved for offline analysis with Origin or custom Matlab software. Cell-attached and whole-cell recording configuration were achieved in voltage-clamp mode, and recordings were subsequently made in current-clamp mode. Whole-cell recordings were compensated by a minimum of 80% with < 10 μs lag, and were discarded if series resistance changed by more than 15% from its initial value. In the attempt to initiate action potentials, current injections were made in six steps (1–6 nA) via the patch electrode. To ensure that voltage-sensitive sodium channels were not in a chronic inactivated state, the recording configuration was periodically turned back to voltage-clamp mode and the cell was held at a potential of −60 mV or less in order to de-inactivate sodium channels. If reliable action potential-like firing was observed in a cell, the broad-spectrum antagonist zonisamide (10 μM; Ascent) or the fast acting sodium channel tetrodotoxin (1 μM) was added to the perfusate.

Results

OCT4 direct conversion reprogramming facilitates generation of a proliferative neural progenitor phenotype from fibroblasts

In an effort to assess the functional conversion capacity of *OCT4* expressing cells, we devised a culture strategy incorporating elements from our previous direct conversion approach using *OCT4*, and the derivation of neural progenitors (NPCs) from pluripotent stem cells (Fig. 1A) [18,19]. Adult hFib transduced with lentivirus expressing *OCT4* were cultured in reprogramming media (R) (hFibR^{OCT4}) for 1 week to enable sufficient expansion of transduced cells (Fig. 1B). hFibR^{OCT4} were then trypsinized to form a single-cell suspension and seeded in neural progenitor culture media. Single-cell suspensions of hFibR^{OCT4} maintained in neural progenitor culture formed neural sphere-like clusters similar to those described from pluripotent cells (Fig. 1C) [19]. To address whether these spheres were a result of proliferation rather than coalescence of cells, we dissociated the spheres and performed cell-cycle analysis using Ki67, a marker of all stages of the active cell cycle. Ki67 expression was evident in a defined subset of sphere-derived cells, of which nearly all cells co-expressed OCT4 (Fig. 1D). Since proliferation is a property of NPCs (Supplementary Fig. S1A; Supplementary Data are available online at www.liebertpub.com/scd), we asked whether hFibR^{OCT4} sphere-derived cells also expressed key neural progenitor regulators. Given that recent reports suggest *SOX2*, a key regulator of NPCs (Supplementary Fig. S1A), is sufficient to induce direct conversion of mouse and human fetal fibroblasts to neural progenitors [20], we analyzed adult-derived hFibR^{OCT4} cells for SOX2 expression. A small but distinct population of cells expressed SOX2, of which nearly all co-expressed OCT4, indicating that *OCT4* expression in conjunction with neural progenitor culture can induce hallmarks of a neural progenitor phenotype (Fig. 1E). Further analysis of hFibR^{OCT4} for the expression of additional neural progenitor markers revealed a subset of OCT4-positive cells that co-expressed the cell surface marker CD133 (Fig. 1F). In addition to these protein-level analyses, hFibR^{OCT4} also displayed up-regulation of *MSI2* and *NCAN* transcript compared with hFibs (Supplementary Fig. S1C). Importantly, hFibR^{OCT4} down-regulated key fibroblast genes *COL1A1*, *DKK3*, and *SNAI1* in response to the reprogramming process (Supplementary Fig. S1D). Taken together, these results demonstrate that hFibR^{OCT4} sphere-derived cells have initiated a molecular shift from fibroblastic programs toward that which reflects well-characterized primary human NPCs [21].

To further characterize these emerging neural-like cells from hFibR^{OCT4} cells, we cultured them on the neural substrate poly-ornathine/laminin (POL). hFibR^{OCT4} sphere-derived cells cultured on POL displayed a similar morphology to NPCs derived from pluripotent cells (Fig. 1F and Supplementary Fig. S1B) [22]. In agreement with flow cytometric analysis, immunofluorescence for OCT4 and SOX2 revealed co-expressing populations of cells organized in colony-like regions consistent with an emerging progenitor phenotype (Fig. 1G). Continued passaging on laminin resulted in linear growth on an exponential scale, indicating that the proliferating population of cells had become

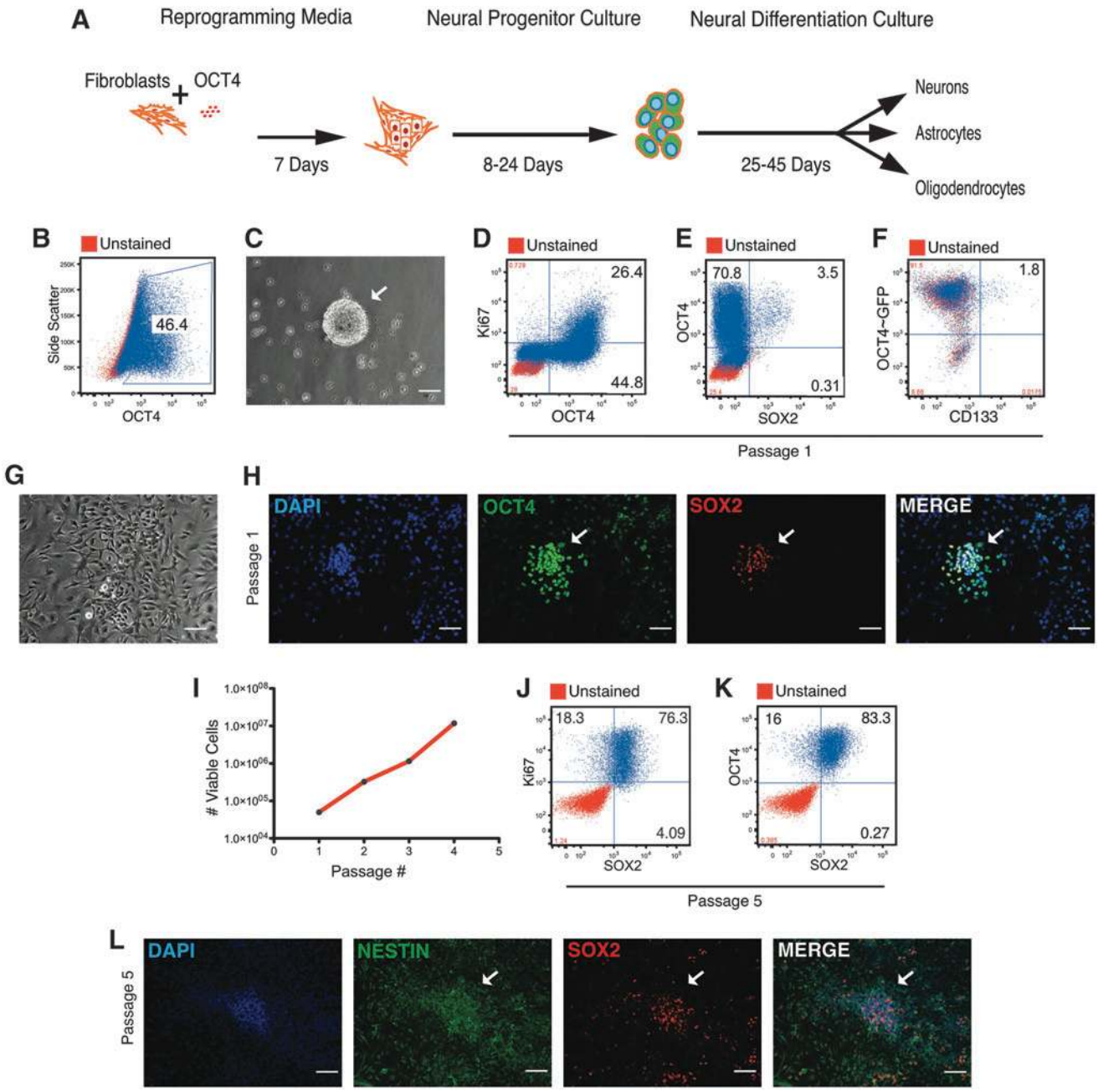

FIG. 1. Expression of *OCT4* in combination with neural progenitor culture induces conversion of fibroblasts to a proliferating neural progenitor-like cell (hFib-NPC^{OCT4}). **(A)** Schematic of conversion strategy. **(B)** Flow cytometric plot of intracellular OCT4 expression in adult human fibroblasts after 8 days of culture in reprogramming media culture (hFibR^{OCT4}). **(C)** Phase-contrast image of hFibR^{OCT4} neural sphere-like clusters after 14 days in neural progenitor culture. **(D)** Flow cytometric plot of OCT4 versus Ki67 expression in hFibR^{OCT4} sphere-derived cells. **(E)** Flow cytometric plot of OCT4 versus SOX2 expression in hFibR^{OCT4} sphere-derived cells. **(F)** Flow cytometric plot of eGFP expression from hFibR^{OCT4} cells generated with pHIV-ef1α-OCT4-IRES-eGFP versus CD133 on live cells. **(G)** Phase-contrast image of hFibR^{OCT4} sphere-derived cells cultured on poly-ornathine/laminin (POL). **(H)** Immunofluorescence results for OCT4 and SOX2 expression in hFibR^{OCT4} sphere-derived cells cultured on POL. **(I)** Cell growth curve illustrating cumulative number of viable trypan blue excluding cells with increasing passage number. **(J)** Flow cytometric plot of SOX2 versus Ki67 expression in passage 5 POL cultured hFibR^{OCT4} sphere-derived cells. **(K)** Flow cytometric plot of OCT4 versus SOX2 expression in passage 5 POL cultured hFibR^{OCT4} sphere-derived cells. **(L)** Immunofluorescence results for NESTIN and SOX2 expression in passage 5 POL cultured hFibR^{OCT4} sphere-derived cells. Representative results from $n = 4$ rounds of hFib-NPC^{OCT4} conversion. Scale bar = 100 μM. *White arrows* denote areas of interest.

abundant (Fig. 1H). Consistent with this observation as well as with expansion of the neural progenitor phenotype, nearly all of the cells in culture expressed the proliferation marker Ki67 in combination with SOX2 (Fig. 1I). Moreover, the vast majority of cells co-expressed OCT4 and SOX2, a clear indication that passaging of hFibR^{OCT4} on laminin had enriched for this phenotype (Fig. 1J). Despite being highly proliferative and expressing the pluripotency-associated transcription factors OCT4 and SOX2, hFibR^{OCT4} cells failed to produce teratomas (or tumors of any kind) when injected into immune-deficient mice at cell concentrations well above the tumor initiating requirement of iPSC (Supplementary Fig. S2A, B). Having verified the absence of pluripotency, we assessed whether the expansion of this phenotype occurred alongside up-regulation of additional neural stem/progenitor marks. Accordingly, we performed immunofluorescence for SOX2 in combination with the neural filament NESTIN, a marker of primitive neural stem/progenitor cells. This analysis revealed co-expression of both SOX2 and NESTIN within hFibR^{OCT4} cells (Fig. 1K). Cumulatively, these results demonstrate that culturing of hFibR^{OCT4} cells in neural progenitor culture is sufficient to confer both growth and phenotypic properties of neural stem/progenitor cells. As such, we termed these cells hFib-NPC^{OCT4}.

To determine whether *OCT4* expression was required to induce direct conversion of adult hFib to NPCs, we cultured *eGFP* expressing fibroblasts using the strategy highlighted in Fig. 1A. Similar to hFibR^{OCT4}, hFibR^{eGFP} were propagated in reprogramming media to expand eGFP expressing cells (Supplementary Fig. S3A). hFibR^{eGFP} were then seeded as single cells in progenitor culture media and analyzed for sphere formation. Surprisingly, hFibR^{eGFP} in these conditions formed sphere-like clusters similar in morphology to hFibR^{OCT4} (Supplementary Fig. S3B). However, cell-cycle analysis of the resulting spheres revealed a comparatively small number of Ki67-positive cells to that of hFibR^{OCT4} spheres (Supplementary Fig. S3C). In addition to the lack of proliferation, hFibR^{eGFP} sphere-derived cells failed to up-regulate the neural stem/progenitor transcription factor SOX2 (Supplementary Fig. S3D), and they displayed fibroblastic morphology after culturing on laminin (Supplementary Fig. S3E). Together, these results indicate that culturing of adult hFib in neural progenitor media is insufficient to sustain

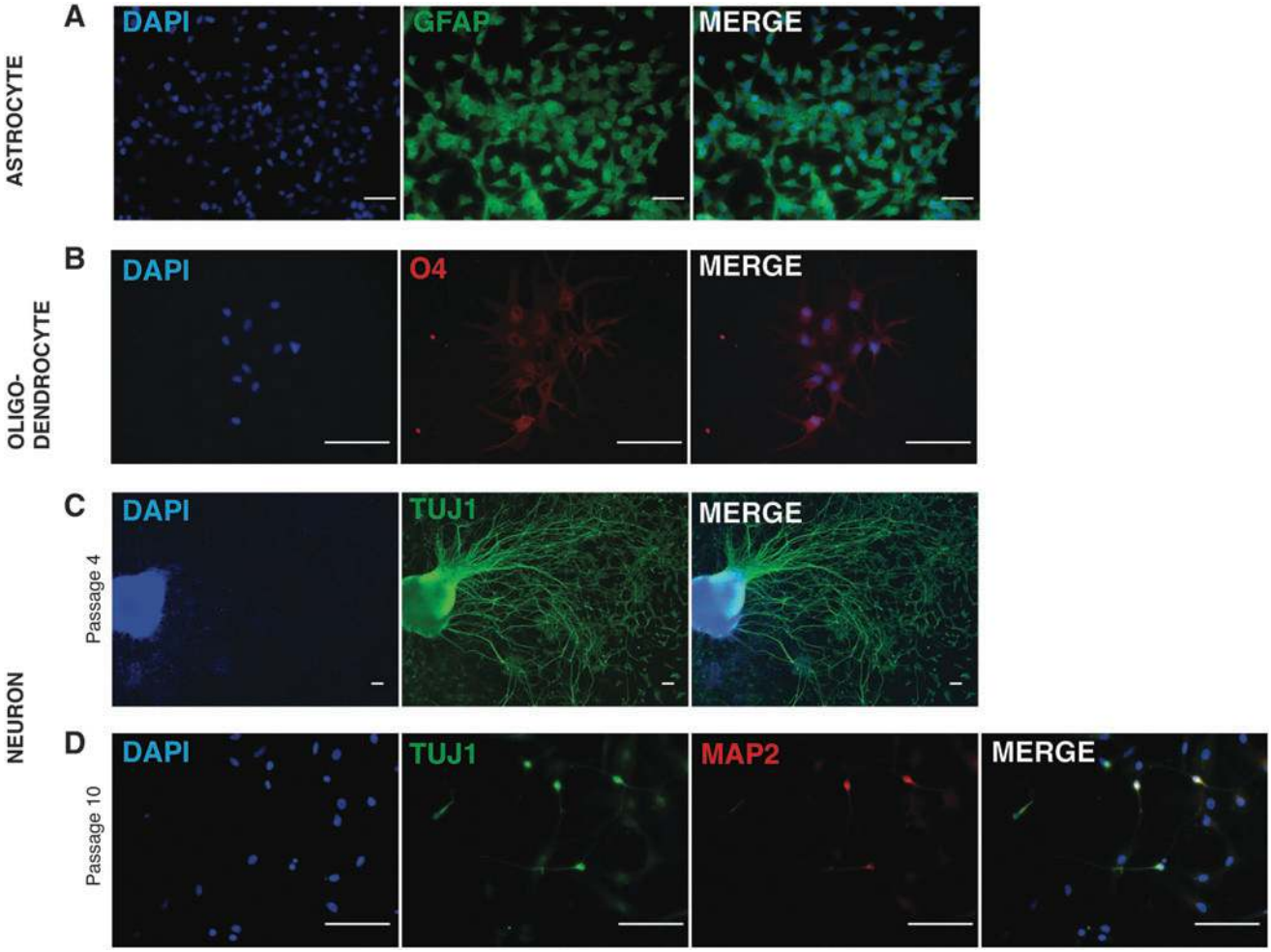

FIG. 2. hFib-NPC^{OCT4} display tri-potent differentiation potential. **(A–D)** Immunofluorescence images of neural lineage protein expression **(A),** GFAP expressing astrocytes. **(B)** O4 expressing oligodendrocytes. **(C)** TUJ1 expressing neurons. **(D)** TUJ1 MAP2 co-expression in a subset of neurons. Representative images from $n=4$ rounds of hFib-NPC^{OCT4} conversion. Scale bar = 100 μM.

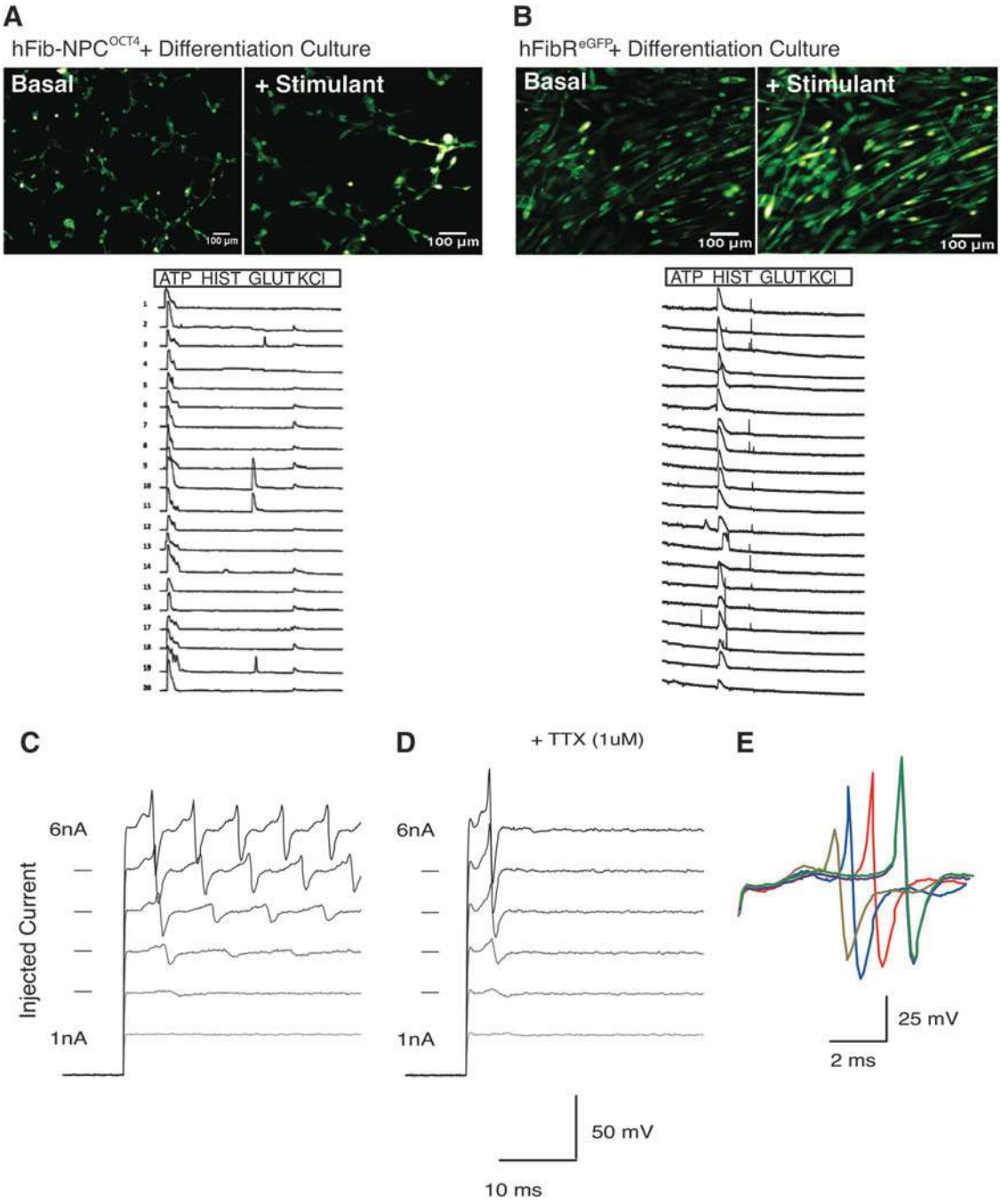

FIG. 3. Differentiated hFib-NPC^{OCT4}-derived neurons demonstrate functional response to neurotransmitters and current injection. **(A)** hFib-NPC^{OCT4} differentiated cells treated with calcium reactive compound FLUO-4 and various calcium release stimuli. Representative fluorescent microscopy images of FLUO-4 dye reacting with calcium after administration with neurotransmitter glutamate. Fluorescent intensity cell trace diagrams of individual cells and cell–cell junctions during treatment with intracellular calcium release stimulants. **(B)** Fibroblasts cultured in neural progenitor and neural differentiation medium treated with FLUO-4 and assayed for calcium release using stimulants. Representative fluorescent microscopy images of FLUO-4 dye reacting with calcium after administration with histamine. Fluorescent intensity cell trace diagrams of individual cells and cell–cell junctions during treatment with intracellular calcium release stimulants. **(C)** Action potential measurements of hFib-NPC^{OCT4}-derived neurons. **(D)** Action potential measurement during administration of fast acting sodium channel inhibitor tetrodotoxin (TTX). **(E)** Averaged traces of evoked repetitive action potentials in four separate cells.

growth and phenotypic characteristics of induced human neural progenitors.

OCT4-NPC differentiate to all three neural subfamilies, including iNs

Although neural progenitor phenotype is defined by the expression of specific transcription factors and structural proteins, progenitor function is assessed in part by the ability to differentiate to the three major families of neural cells: neurons, astrocytes, and oligodendrocytes. Differentiation of neural stem/progenitors can be achieved by withdrawal of factors shown to support proliferation and addition of those that support the generation of specific lineages of neural cells (Supplementary Fig. S4) [22]. Accordingly, the culturing of hFib-NPC^{OCT4} in differentiation conditions shown to support the generation of glial cells produced glial fibrilliary acidic protein expressing cells resembling astrocytes (Fig. 2A) and O4 expressing cells resembling oligodendrocytes (Fig. 2B). Moreover, culturing of hFib-NPC^{OCT4} in neuronal differentiation media was able to induce the generation of a neuronal phenotype, marked by expression of the neuron-specific class III beta-tubulin protein or TUJ1 (Fig. 2C). Further exposure of hFib-NPC^{OCT4}-derived neurons to differentiation media resulted in the formation of a subset of TUJ1-positive neurons that up-regulated the mature neuronal marker MAP2 (Fig. 2D). Importantly, cells which expressed high levels of TUJ1 also demonstrated little to no expression of OCT4, suggesting that differentiation toward mature functional cell types occurs concomitantly with silencing of *OCT4* expression (Supplementary Fig. S5A, B).

To assess the functional capacity of hFib-NPC^{OCT4}-derived mature neurons, we evaluated their response to the neurotransmitters ATP and glutamate via calcium transient formation using a FLUO-4 fluorescence assay. Nearly all hFib-NPC^{OCT4}-derived neurons produced calcium transients in response to ATP, while a distinct subset responded to glutamate. Importantly, hFib-NPC^{OCT4} neurons did not respond to histamine, a known inducer of calcium release in fibroblasts (Fig. 3A, B). Furthermore, hFib-NPC^{OCT4}-derived neurons fired repetitive action potentials in response to a current injection, and exhibited sensitivity to a sodium channel inhibitor (Fig. 3C–E). These collective results suggest that hFib-NPC^{OCT4} possess all of the defining features of tri-potent NPCs, confirming successful cell fate transition through the expression of *OCT4*.

OCT4 expression activates a hierarchy of neural conversion transcription factors during reprogramming of adult hFib to NPC

Having confirmed that hFib-NPC^{OCT4} possess both phenotypic and developmental characteristics of NPCs, we next aimed at better understanding the molecular events underlying the reprogramming process. Given that hFib-NPC^{OCT4} express SOX2, a neural fate conversion factor, we investigated whether other genes shown to induce neural fate were similarly activated during the reprogramming process. We performed qRT-PCR on Fibs, hFibR^{eGFP}, and hFibR^{OCT4} sphere-derived cells to measure the expression of genes shown to induce the neural fate from fibroblasts: *BRN-2*, *ASCL1*, *MYT1L*, and *NEUROD1* (Fig. 4A–D). With the exception of *ASCL1*, hFibR^{OCT4} progenitor culture demonstrated elevated expression of neural conversion genes compared with naïve fibroblasts and hFibR^{eGFP} progenitor culture. Based on these results and the induced expression of *SOX2*, we hypothesized that the combination of *OCT4* and neural progenitor culture may regulate a hierarchy of established transcriptional networks for converting fibroblasts to the neural lineage. Considering recent reports, we postulated

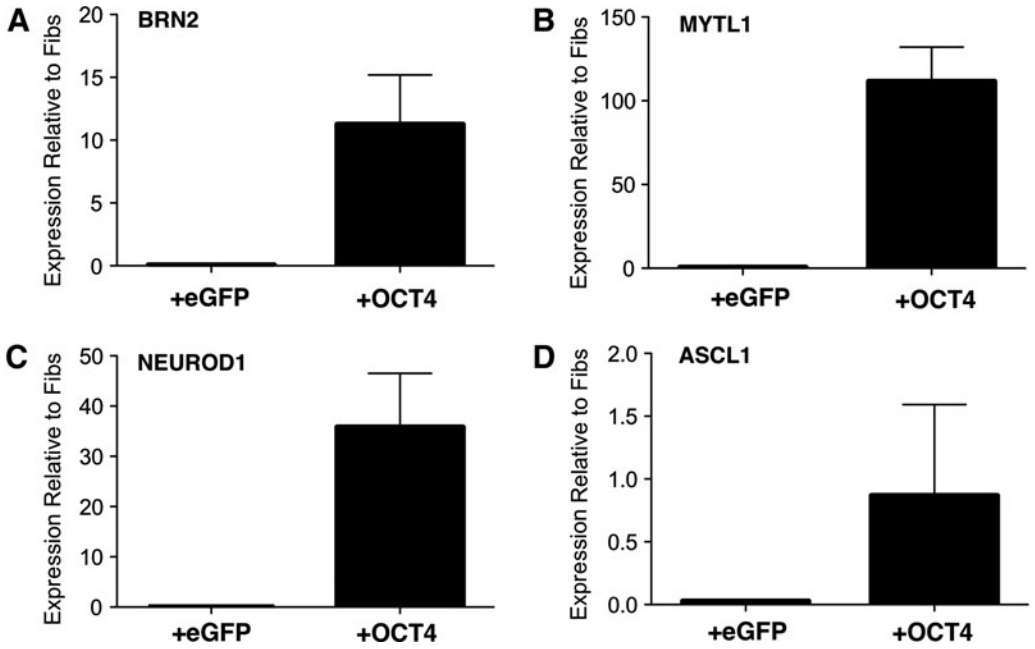

FIG. 4. hFib-NPC^{OCT4} activate neural conversion transcription factors. **(A–D)** qRT-PCR results for expression of neural conversion transcription factors in hFibR^{eGFP} cultured in neural progenitor culture, and hFibR^{OCT4} cultured in neural progenitor culture. Expression levels are normalized to expression in hFibs.

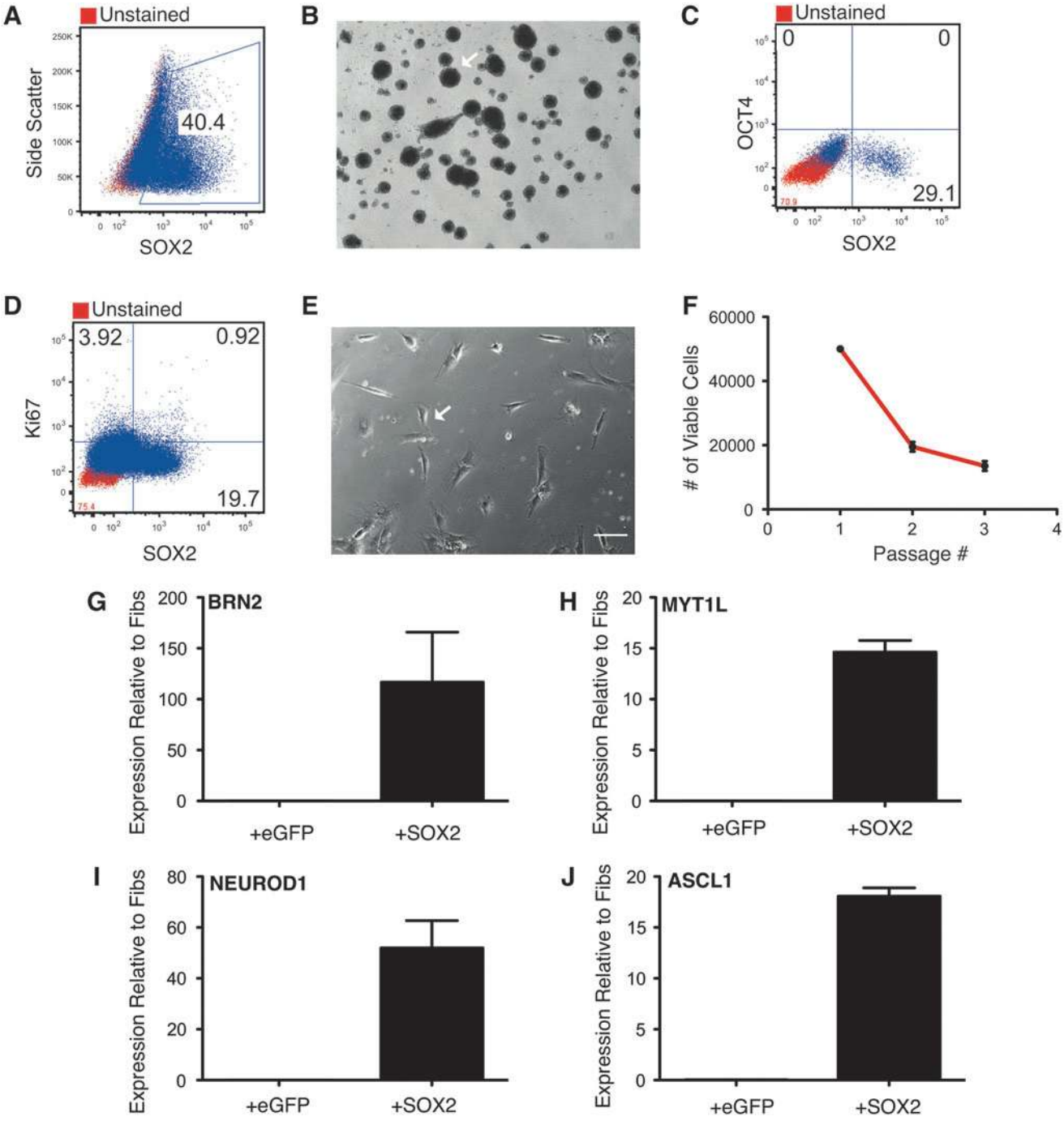

FIG. 5. Expression of *SOX2* in combination with neural progenitor culture fails to induce conversion of adult fibroblasts to neural progenitors, despite successfully activating downstream neural conversion transcription factors. **(A)** Flow cytometric plot of intracellular SOX2 expression in adult human fibroblasts after 8 days in reprogramming media (hFibR^{SOX2}). **(B)** Phase-contrast image of hFibR^{SOX2} sphere-like clusters after 14 days in neural progenitor culture. **(C)** Flow cytometric plot of SOX2 versus OCT4 expression in hFibR^{SOX2} sphere-derived cells. **(D)** Flow cytometric plot of SOX2 versus Ki67 expression in hFibR^{SOX2} sphere-derived cells. **(E)** Phase-contrast image of hFibR^{SOX2} sphere-derived cells cultured on POL. **(F)** Cell growth curve illustrating cumulative number of viable trypan blue excluding cells with increasing passage number. **(G–J)** qRT-PCR results for expression of neural conversion transcription factors in hFib^{eGFP} cultured in neural progenitor culture, and hFibR^{SOX2} cultured in neural progenitor culture. Expression levels are normalized to expression in hFibs ($n = 2$). Representative results from $n = 3$ attempts of hFibR^{SOX2} conversion. *White arrows* indicate areas of interest.

that *SOX2* should act downstream of *OCT4*, and, therefore, should be able to convert adult hFib to neural progenitors in the absence of *OCT4*. To test this hypothesis, we transduced adult hFib with lentivirus expressing *SOX2* and cultured them according to the strategy in Fig. 1A. hFibR^{SOX2} were cultured in reprogramming media to enable expansion of SOX2 expressing cells (Fig. 5A). hFibR^{SOX2} cells were seeded as single cells in neural progenitor culture media and analyzed for sphere formation. After 2 weeks in neural progenitor culture, hFibR^{SOX2} single cells had given rise to neural sphere-like clusters similar to hFibR^{OCT4} (Fig. 5B). Although forced expression of *OCT4* was able to up-regulate expression of SOX2 (Fig. 1E), forced expression of *SOX2* did not up-regulate OCT4 (Fig. 5C). Similar to hFibR^{eGFP}, hFibR^{SOX2} sphere-like clusters contained low percentages of Ki67-positive proliferating cells (Fig. 5D). Moreover, propagation of hFibR^{SOX2} sphere-derived cells on the neural substrate laminin resulted in the generation of cells with fibroblastic morphologies (Fig. 5E), and a sharp decline in cell viability (Fig. 5F). Despite the failure of hFibR^{SOX2} to propagate in neural supportive culture conditions, qRT-PCR analysis displayed a similar pattern to hFibR^{OCT4} regarding the up-regulation of *BRN-2*, *MYT1L*, and *NEUROD1* (Fig. 5G–J). These results suggest that *SOX2* expression is activated in response to *OCT4* expression, and that *SOX2* expression is sufficient to activate neural fate conversion factors *BRN-2*, *MYT1L*, *ASCL1*, and *NEUROD1*. However, forced expression of *SOX2* alone is not sufficient to induce neural progenitor fate from adult hFib, suggesting a unique additional role for *OCT4* during the reprogramming process.

Reprogramming technologies are seen to hold great potential for the construction of patient-specific disease models and cells for drug screening. However, in order to ensure applicability of a given reprogramming technology to patient-specific endeavors, freshly derived cell cultures from donors should prove to be a suitable starting material for successful cell fate transition. To ensure that hFib-NPC^{OCT4} reprogramming was applicable to donor-derived fibroblasts, we generated hFib-NPC^{OCT4} cells from a freshly isolated skin biopsy [hFib(2)]. hFibR(2)^{OCT4} formed spheres in neural progenitor culture media, and on dissociation were able to propagate on the neural substrate laminin (Supplementary Fig. S6A). Laminin-adapted hFibR(2) sphere-derived cells displayed a similar morphology to hFibR^{OCT4} sphere-derived cells and NPCs derived from ESCs (Fig. 1G and Supplementary Fig. S1B). Importantly, hFibR(2)^{OCT4} sphere-derived cells activated established neural conversion factors in an *OCT4*-dependent manner, suggesting that they had established similar neural conversion regulatory networks as hFib-NPC^{OCT4} (Supplementary Fig. S6B). Furthermore, when cultured in neural differentiation conditions, hFibR(2)^{OCT4} cells successfully differentiated to all three major subfamilies of neural cells, including astrocytes, oligodendrocytes, and neurons (Supplementary Fig. S6C). Taken together, these results confirm that hFib-NPC^{OCT4} reprogramming is applicable to multiple lines of adult fibroblasts, illustrating the robust nature of *OCT4* to alter cell fate.

Discussion

Derivation of hFib-NPC^{OCT4} is simple, rapid, and produces a proliferative, nontumorgenic population of progenitor cells that are capable of differentiating to all three major neural subtypes: neurons, astrocytes, and oligodendrocytes. Importantly, hFib-NPC^{OCT4}-derived neurons functionally respond to both current injection and neurotransmitters, positioning hFib-NPC^{OCT4} as an appealing reprogramming tool for the generation of neuronal-based disease models in a manner that is not convoluted by the use of other factors associated with stages of neural development [23] or promiscuous chemical manipulation in vitro [24]. This reprogramming technology is sufficiently robust and enables the use of donor-derived adult fibroblasts as a starting material for cell fate conversion, positioning it as a candidate for the construction of relevant patient-specific disease models for use in drug screening.

Our study represents the only example where a single exogenous factor, *OCT4*, has directly reprogrammed adult human somatic cells to tri-potent neural progenitors without other manipulations. Although co-expression of *SOX2* hallmarks the emergence of hFib-NPC^{OCT4}, expression of *SOX2* alone in adult hFib using our culture system does not result in successful reprogramming to neural progenitors. However, forced expression of *SOX2* in the presence of a feeder support layer has been shown to induce direct conversion of human fetal fibroblasts to tri-potent NPCs [20]. Therefore, it is likely that the required (yet undefined) regulation bestowed by the feeder layer on cells undergoing *SOX2* neural cell fate conversion is intrinsic to cells undergoing *OCT4*-induced neural cell fate conversion. The up-regulation of key neural conversion factors during reprogramming of fibroblasts to hFib-NPC^{OCT4} in this study is not unlike the up-regulation of key hematopoietic transcription factors reported during the conversion of fibroblasts to multipotent blood progenitors using *OCT-4* alone [18]. Together, these findings highlight the acquisition of crucial fate-inducing transcriptional programs as a result of forced *OCT-4* expression in hFib that may also enable other cell fates to be induced. These and other lineage-based studies are currently ongoing in our lab.

Acknowledgments

The authors would like to thank Tony Collins and Luca Orlando for a critical review of this article as well as Nick Holzapfel and Kristin Hope for MSI2 primer sequences. R.R.M is funded by CIHR (Alexander Graham Bell Graduate Scholarship). E.S. is funded by MITACS during her involvement with these studies. Y.D.B is funded by CIHR. J.A. is funded by CONACyT fellowship. D.C.G. is funded by CIHR and Ontario Early Researcher Award. M.B. is funded by CIHR operating grants and Boris Foundation. Portions of this material were presented at ISSCR Roddenberry International Symposium on Cellular Reprogramming October 2012.

Author Disclosure Statement

The authors declare that there are no conflicts of interest.

References

1. Weintraub H, SJ Tapscott, RL Davis, MJ Thayer, MA Adam, AB Lassar and AD Miller. (1989). Activation of muscle-specific genes in pigment, nerve, fat, liver, and fibroblast cell lines by forced expression of MyoD. Proc Natl Acad Sci U S A 86:5434–5438.

2. Sancho-Martinez I, SH Baek and JC Izpisua Belmonte. (2012). Lineage conversion methodologies meet the reprogramming toolbox. Nat Cell Biol 14:892–899.
3. Vierbuchen T and M Wernig. (2012). Molecular roadblocks for cellular reprogramming. Mol Cell 47:827–838.
4. Orkin SH and K Hochedlinger. (2011). Chromatin connections to pluripotency and cellular reprogramming. Cell 145:835–850.
5. Vierbuchen T, A Ostermeier, ZP Pang, Y Kokubu, TC Sudhof and M Wernig. (2010). Direct conversion of fibroblasts to functional neurons by defined factors. Nature 463:1035–1041.
6. Qiang L, R Fujita, T Yamashita, S Angulo, H Rhinn, D Rhee, C Doege, L Chau, L Aubry, et al. (2011). Directed conversion of Alzheimer's disease patient skin fibroblasts into functional neurons. Cell 146:359–371.
7. Pfisterer U, A Kirkeby, O Torper, J Wood, J Nelander, A Dufour, A Bjorklund, O Lindvall, J Jakobsson and M Parmar. (2011). Direct conversion of human fibroblasts to dopaminergic neurons. Proc Natl Acad Sci U S A 108: 10343–10348.
8. Son EY, JK Ichida, BJ Wainger, JS Toma, VF Rafuse, CJ Woolf and K Eggan. (2011). Conversion of mouse and human fibroblasts into functional spinal motor neurons. Cell Stem Cell 9:205–218.
9. Marro S, ZP Pang, N Yang, MC Tsai, K Qu, HY Chang, TC Sudhof and M Wernig. (2011). Direct lineage conversion of terminally differentiated hepatocytes to functional neurons. Cell Stem Cell 9:374–382.
10. Caiazzo M, MT Dell'Anno, E Dvoretskova, D Lazarevic, S Taverna, D Leo, TD Sotnikova, A Menegon, P Roncaglia, et al. (2011). Direct generation of functional dopaminergic neurons from mouse and human fibroblasts. Nature 476: 224–227.
11. Kim J, JA Efe, S Zhu, M Talantova, X Yuan, S Wang, SA Lipton, K Zhang and S Ding. (2011). Direct reprogramming of mouse fibroblasts to neural progenitors. Proc Natl Acad Sci U S A 108:7838–7843.
12. Thier M, P Worsdorfer, YB Lakes, R Gorris, S Herms, T Opitz, D Seiferling, T Quandel, P Hoffmann, et al. (2012). Direct conversion of fibroblasts into stably expandable neural stem cells. Cell Stem Cell 10:473–479.
13. Sheng C, Q Zheng, J Wu, Z Xu, L Wang, W Li, H Zhang, XY Zhao, L Liu, et al. (2012). Direct reprogramming of Sertoli cells into multipotent neural stem cells by defined factors. Cell Res 22:208–218.
14. Lujan E, S Chanda, H Ahlenius, TC Sudhof and M Wernig. (2012). Direct conversion of mouse fibroblasts to self-renewing, tripotent neural precursor cells. Proc Natl Acad Sci U S A 109:2527–2532.
15. Han DW, N Tapia, A Hermann, K Hemmer, S Hoing, MJ Arauzo-Bravo, H Zaehres, G Wu, S Frank, et al. (2012). Direct reprogramming of fibroblasts into neural stem cells by defined factors. Cell Stem Cell 10:465–472.
16. Villegas J and M McPhaul. (2005). Establishment and culture of human skin fibroblasts. Curr Protoc Mol Biol Chapter 28:Unit 28 3.
17. Werbowetski-Ogilvie TE, M Bosse, M Stewart, A Schnerch, V Ramos-Mejia, A Rouleau, T Wynder, MJ Smith, S Dingwall, et al. (2009). Characterization of human embryonic stem cells with features of neoplastic progression. Nat Biotechnol 27:91–97.
18. Szabo E, S Rampalli, RM Risueno, A Schnerch, R Mitchell, A Fiebig-Comyn, M Levadoux-Martin and M Bhatia. (2010). Direct conversion of human fibroblasts to multilineage blood progenitors. Nature 468:521–526.
19. Carpenter MK, MS Inokuma, J Denham, T Mujtaba, CP Chiu and MS Rao. (2001). Enrichment of neurons and neural precursors from human embryonic stem cells. Exp Neurol 172:383–397.
20. Ring KL, LM Tong, ME Balestra, R Javier, Y Andrews-Zwilling, G Li, D Walker, WR Zhang, AC Kreitzer and Y Huang. (2012). Direct reprogramming of mouse and human fibroblasts into multipotent neural stem cells with a single factor. Cell Stem Cell 11:100–109.
21. Schwartz PH, PJ Bryant, TJ Fuja, H Su, DK O'Dowd and H Klassen. (2003). Isolation and characterization of neural progenitor cells from post-mortem human cortex. J Neurosci Res 74:838–851.
22. Werbowetski-Ogilvie TE, LC Morrison, A Fiebig-Comyn and M Bhatia. (2012). *In vivo* generation of neural tumors from neoplastic pluripotent stem cells models early human pediatric brain tumor formation. Stem Cells 30:392–404.
23. Wapinski OL, T Vierbuchen, K Qu, QY Lee, S Chanda, DR Fuentes, PG Giresi, YH Ng, S Marro, et al. (2013). Hierarchical mechanisms for direct reprogramming of fibroblasts to neurons. Cell 155:621–635.
24. Zhu S, R Ambasudhan, W Sun, HJ Kim, M Talantova, X Wang, M Zhang, Y Zhang, T Laurent, et al. (2014). Small molecules enable OCT4-mediated direct reprogramming into expandable human neural stem cells. Cell Res 24: 126–129.

Address correspondence to:
Dr. Mickie Bhatia
Faculty of Health Sciences
Stem Cell and Cancer Research Institute
McMaster University
1200 Main Street West, MDCL 5029
Hamilton, ON L8N 3Z5
Canada

E-mail: mbhatia@mcmaster.ca

Received for publication January 10, 2014
Accepted after revision March 28, 2014
Prepublished on Liebert Instant Online April 2, 2014